Nuclear Medicine and Biology 41 (2014) e44–e48

Contents lists available at ScienceDirect

Nuclear Medicine and Biology

journal homepage: www.elsevier.com/locate/nucmedbio

Biodistribution of a ^{67}Ga-labeled anti-TNF VHH single-domain antibody containing a bacterial albumin-binding domain (Zag)

Maurício Morais [a,1], Cátia Cantante [b,c,1], Lurdes Gano [a], Isabel Santos [a], Sara Lourenço [d], Catarina Santos [b,c], Carlos Fontes [e], Frederico Aires da Silva [d], João Gonçalves [b,c], João D.G. Correia [a,*]

[a] Centro de Ciências e Tecnologias Nucleares, Instituto Superior Técnico, Universidade de Lisboa, Estrada Nacional 10, ao km 139.7, 2695–066 Bobadela LRS, Portugal
[b] CPM-URIA Fac. Farmácia, Universidade de Lisboa, Av. Prof. Gama Pinto, 1649–003 Lisboa, Portugal
[c] IMM, Fac. Med., Universidade de Lisboa, Av. Prof. Egas Moniz 1649–028 Lisboa, Portugal
[d] TechnoPhage S.A., Av. Prof. Egas Moniz, Edifício Egas Moniz Piso 2, 1649–028 Lisboa, Portugal
[e] Fac. Med. Veterinária, Universidade de Lisboa, Av. da Universidade Técnica 1300–477 Lisboa, Portugal

ARTICLE INFO

Article history:
Received 27 September 2013
Received in revised form 3 January 2014
Accepted 10 January 2014

Keywords:
Albumin-binding domain
Biodistribution
Gallium-67
Plasma half-life
Single-domain antibodies

ABSTRACT

Introduction: Small domain antibodies (sdAbs) present high potential for both molecular *in vivo* imaging and therapy. Owing to the low molecular weight they are rapidly cleared from blood circulation, and new strategies to extend their half-lifes are needed for therapeutic applications. We have selected a bacterial albumin-binding domain (ABD) from protein Zag to be fused to an anti-tumor necrosis factor (TNF) single variable-domain heavy-chain region antibody (VHH) to delay blood clearance, and evaluated the biodistribution profile of the fusion protein.

Methods: The anti-TNF VHH and the fusion protein VHH-Zag were conjugated to S-2-(4-isothiocyanatobenzyl)-1,4,7-triazacyclononane-1,4,7-triacetic acid (p-SCN-Bn-NOTA). The anti-TNF and albumin-binding properties of the conjugates NOTA-VHH and NOTA-VHH-Zag were assessed by enzyme-linked immunosorbent assay (ELISA). The radioconjugates ^{67}Ga-NOTA-VHH and ^{67}Ga-NOTA-VHH-Zag were obtained by reaction of $^{67}GaCl_3$ with the corresponding conjugates at room temperature. Biodistribution studies were performed in healthy female CD-1 mice.

Results: The immunoreactivity of the VHH-based proteins is preserved upon conjugation to NOTA as well as after radiometallation. The radiochemical purity of the radioconjugates was higher than 95% as determined by ITLC-SG after purification by gel filtration. The biodistribution studies showed that the Zag domain affected the pharmacokinetic properties of VHH, with impressive differences in blood clearance (0.028 ± 0.004 *vs* 1.7 ± 0.8 % I.A./g) and total excretion (97.8 ± 0.6 *vs* 25.5 ± 2.1 % I.A.) for ^{67}Ga-NOTA-VHH and ^{67}Ga-NOTA-VHH-Zag, respectively, at 24 h p.i.

Conclusion: The Zag domain prolonged the circulation time of VHH by reducing the blood clearance of the labeled fusion protein ^{67}Ga-NOTA-VHH-Zag. In this way, the anti-TNF VHH in fusion with the Zag ABD presents a higher therapeutic potential than the unmodified VHH.

1. Introduction

The great majority of therapeutic antibodies marketed are full-length Immunoglobulin G (IgG) molecules that trigger effector functions and present long serum half-life [1]. Indeed, their high molecular weight (~150 kDa) leads to long residence time in blood circulation. Additionally, IgG antibodies diffuse poorly into solid tumors, and clear slowly from the body [1]. Despite their recognized potential for *in vivo* imaging applications, those features lead to poor contrast, which strongly hampers the wide use of antibodies as tracers for target-specific molecular imaging [2,3]. The same holds true for targeted radionuclide therapy of solid tumors using immunoglobulins. Indeed, the long half-life results in irradiation of non-target organs and tissues, and slow extravasation and penetration into the tumor, limiting the radiotherapeutic effect [3,4]. Overall, the drawbacks associated to IgGs, together with the rapid progress in recombinant technologies led to the development of smaller engineered antibodies and proteins, such as single-chain variable fragments (scFvs), sdAbs and affibodies [1–5]. However, due to their lower molecular weight, these proteins present in general significantly shorter half-lifes and very rapid blood clearance, which hampers therapeutic applications, e.g. requiring infusions or repeated injections to maintain a therapeutically effective dose over a prolonged period of time [6]. Aiming to address this issue, several approaches have been proposed to extend plasma half-lifes of therapeutic proteins and, consequently, improve their overall

* Corresponding author. Tel.: +351 21 994 62 33.
E-mail address: jgalamba@itn.pt (J.D.G. Correia).
[1] These authors contributed equally to the article.

0969-8051/$ – see front matter © 2014 Elsevier Inc. All rights reserved.
http://dx.doi.org/10.1016/j.nucmedbio.2014.01.009

biological properties. Some of these strategies aim at increasing the hydrodynamic volume of the molecules, thus reducing renal filtration and degradation. Among the various explored approaches, the noncovalent association of a therapeutic protein to plasma proteins, namely to albumin, or fusion of ABDs, peptides or low-molecular-weight albumin binders emerged as quite promising [7–10]. Human serum albumin (HSA) is the most abundant blood plasma protein and is produced in the liver as a monomeric protein of 67 kDa. Albumin presents an extraordinary long circulation half-life of approximately 19 days in humans and 3 days in mice, as a direct result of its size and interaction with the FcRn mediated recycling pathway [8,11]. Furthermore, HSA accumulates in tumors as well as arthritic joints and is a valuable biomarker of many diseases, including cancer, rheumatoid arthritis, and ischemia, among others [11].

ABDs have also been used for improvement of the biological properties of radiolabeled affibodies for systemic radiotherapy, with remarkable reduction of renal accumulation of radioactivity [10,12,13]. More recently, Müller et al. reported a ^{177}Lu-labeled folate conjugate containing an albumin-binding group (4-(*p*-iodophenyl) butyric acid derivative), which presented a significant increase of the tumor-to-kidney ratio of radioactivity compared to the radioconjugate were the albumin-binding group is absent.

We and others have been exploiting bacterial ABDs fused to antibody fragments to prolong the half-life of the resulting fusion proteins [7,8,14,15].

The study presented herein aims at assessing the biodistribution profile of an anti-TNF VHH fused to the Zag ABD (VHH-Zag) isolated from Zag protein, which is a G-related protein from the surface of *Streptococcus zooepidemicus* [16]. To achieve this goal, the fusion protein was conjugated to p-SCN-Bn-NOTA derivative to yield the conjugate NOTA-VHH-Zag, which was labeled with gallium-67 (^{67}Ga). The tissue distribution of the radiolabeled fusion protein (^{67}Ga-NOTA-VHH-Zag) was evaluated in CD-1 mice and the results were compared with those obtained with ^{67}Ga-NOTA-VHH, prepared as control tracer.

2. Materials and methods

SEP-PAK SI cartridges were purchase from Waters. Amicon centrifugal filter (M.W. cut-off = 10 kDa) units and PD-10 columns were purchase from Millipore and GE Healthcare, respectively. Gallium-67 citrate was a gift from the nuclear medicine service of Hospital de Santa Maria (Lisbon, Portugal). Gallium-67 chloride was prepared from Gallium-67 citrate as described in the literature [17]. Diethylenetriaminepentaacetic acid (DTPA) was purchased from Sigma Aldrich. Instant Thin Layer Cromatography (ITLC): Analysis was performed using ITLC-SG Varian and Whatman nº1 strips eluted with the systems:

System A: 2 % HCl 0.5 M in Saline. $^{67}GaCl_3$ migrates in the front of the solvent (Rf = 1), while the radioactive VHH and VHH-Zag stay at the origin (Rf = 0).

System B: 55% MeOH in water. Complex ^{67}Ga-DTPA migrates in the front of the solvent (Rf = 1), $^{67}GaCl_3$ presents some mobility (Rf = 0.4), while the radiolabeled antibody fragments VHH and VHH-Zag stay at the origin (Rf = 0).

Radioactivity distribution on the ITLC strips was detected by a radioactive scanner (Berthold LB 2723, Germany) equipped with 20 mm diameter NaI(Tl) scintillation crystal. Radioactivity measurements were done on a dose calibrator (Aloka Curiemeter, IGC-3, Japan) or on a gamma-counter (Berthold LB 2111, Germany).

2.1. Construction of VHH and VHH-Zag fusion protein

DNA encoding the anti-TNF VHH 3E clone [18] was synthesised by Nzytech adding a *Sfi*I restriction site at 5' and 3' ends, respectively, for cloning into the pComb3x plasmid. pComb3X contains a peptide leader (PL) and sequences encoding peptide tags for purification (6-His) and detection (HA). A fragment encoding the PL-VHH-HIS-HA was generated by PCR and subcloned into the expression vector pT7 (Sigma-Aldrich) into the *Kpn*I and *Hind*III restriction sites. To construct the VHH-Zag fusion, a DNA fragment comprising the entire Zag albumin-binding domain of *Streptococcal* was generated using PCR and adding *Spe*I and *Nco*I restriction sites at the fragment 5' and 3' ends, respectively. The resulting PCR fragments were gel-purified, digested with the *Spe*I and *Nco*I restriction enzymes and cloned into the appropriately cut pT7-PL-VHH-HIS-HA vector. The VHH and VHH-Zag constructs were verified by sequencing.

2.2. Expression and purification of VHH and VHH-Zag

The VHH and VHH fused with the Zag (VHH-Zag) cloned in the pT7 expression vector were expressed in *Escherichia coli* BL21 (DE3) cells. Both VHH and VHH-Zag constructions were confirmed by sequencing. One liter of LB with 100 μg/mL ampicilin was inoculated with 10 mL of overnight culture of transformed BL21 (DE3) and grown to exponential phase (A_{600} = 0,6-0,8) at 37 ºC. Protein expression was induced by addition of 1 mM isopropyl 1-thiol-β-D-galactopyranoside and bacteria were grown 16 h at 18 ºC. Cells were harvested by centrifugation and ressupended in 50 mM HEPES, 1 M NaCl, 5 mM $CaCl_2$, pH 7.5. The pellet was sonicated at 4 ºC during 20 min and centrifuged at 10.000 rpm for 30 min at 4 ºC. Supernatant was purified by immobilized metal affinity chromatography (IMAC), using HP HisTrap columns and the AKTA FPLC system from GE Healthcare [14,15]. After purification, the purity (>95%) of the eluted samples was analyzed by sodium dodecyl sulfate-polyacrylamide gel electrophoresis (SDS-PAGE). The SDS-PAGE analysis of the purified VHH and VHH-Zag samples is presented in Supporting information (Fig. 1S). ExPASy - ProtParam tool was used to estimate the extinction coefficient of VHH and VHH-Zag ($\varepsilon_{\mathbf{VHH}}$ = 34380 L mol^{-1} cm^{-1}; $\varepsilon_{\mathbf{VHH\text{-}Zag}}$ = 38850 L mol^{-1} cm^{-1}).

2.3. Conjugation of p-SCN-Bn-NOTA to VHH and VHH-Zag

The VHH-based antibodies were conjugated to p-SCN-Bn-NOTA as described in the literature [19]. Briefly, VHH or VHH-Zag in 0.05 M sodium carbonate buffer, pH 8.7 (1.5 mL), was added to p-SCN-Bn-NOTA (10-fold molar excess) and incubated for 2 h at room temperature. The coupling reaction was quenched by adjusting the pH to 7.0 – 7.4 using HCl, 1 M. The conjugate was then purified by gel filtration using a HiPrep™ 16/60 Sephacryl™ S-100 High Resolution column purchased from GE Healthcare and 50 mM HEPES, 200 mM NaCl, 5 mM $CaCl_2$, pH 7.5, as eluent. The concentration of NOTA-VHH and NOTA-VHH-Zag was determined at 280 nm using Nanodrop ND-1000 spectrophotometer and the following corrected extinction coefficients: $\varepsilon_{\mathbf{VHH}}$ = 34380 L mol^{-1} cm^{-1}; $\varepsilon_{\mathbf{VHH\text{-}Zag}}$ = 38850 L mol^{-1} cm^{-1} and molecular weights: MW (VHH) = 19.38 kDa; MW(VHH-Zag) = 25.2 kDa.

2.4. Radiolabelling

The pH of a fraction (0.5 mL) of $^{67}GaCl_3$ eluted from a SEP-PAK cartridge was adjusted to 5 by adding sodium acetate up to a 0.26 M concentration. To 150 μL of this solution (20 MBq), NOTA-VHH or NOTA-VHH-Zag (14.3 -16.4 nmol) in 50 μL of acetate buffer (0.1 M, pH = 5) was added and incubated for 5 min at room temperature. The products were purified by gel filtration on a disposable PD10 column. The final solutions were analysed by ITLC: ^{67}Ga-NOTA-VHH, (R_f = 0) using system A and B; ^{67}Ga-NOTA-VHH-Zag (R_f = 0) using system A and B.

2.5. ELISA assay

Human serum albumina (HSA), rat serum albumin (RSA), mouse serum albumin (MSA) (10 μg/well) and human TNFα (200 ng/well) were incubated overnight at 4 ºC in 96-well plate. The remaining binding sites were blocked with 5% (w/v) soya milk/PBS1x during 1 h. The VHH and VHH-Zag recombinant antibodies conjugated with NOTA and the ^{67}Ga-labelled antibodies (after decay – 10 half-lifes) were incubated for 1 h at room temperature. Detection was performed with HRP-conjugated anti-HA-tag antibody (Roche) using ABTS substrate. Absorbance was measured at 405 nm in an ELISA reader.

2.6. DTPA challenge

Aliquots of ^{67}Ga-NOTA-VHH and ^{67}Ga-NOTA-VHH-Zag were added to an aqueous solution of DTPA (900 μL, 10^{-3} M) in a 1:100 molar ratio, and incubated at 37 ºC. The samples were analyzed by ITLC-SG at different time points (2 h, 4 h, 6 h and 24 h) before and after filtration through a disposable PD10 column.

2.7. Biodistribution studies

The *in vivo* biodistribution studies of ^{67}Ga-NOTA-VHH and ^{67}Ga-NOTA-VHH-Zag were performed in groups of 3 healthy female CD-1 mice (Charles River, Spain) weighing approximately 23–25 g each. All animal experiments were performed in accordance with the guidelines for animal care and ethics for animal experiments outlined in the National and European Law. Animals were intravenously injected into the tail vein with 100 μL of the radiolabeled compounds (1.5–3.5 MBq) and were maintained on normal diet ad libitum. At 1 h, 4 h, 24 h post-injection (p.i.) mice were sacrificed by cervical dislocation. The radioactivity administered to the animals was measured using a dose calibrator. The difference between the radioactivity in the injected and that in the killed animals was assumed to be due to total excretion. Tissues of interest were dissected, rinsed to remove excess blood, weighed, and their radioactivity was measured using a gamma counter. Blood and urine was also collected at the sacrifice time and analyzed by ITLC. Biodistribution results were expressed as the percentage of the injected activity per gram of tissue. Statistical analysis of the biodistribution data (t-test) was done with GraphPad Prism and the level of significance was set as 0.05.

3. Results and discussion

In the present study we have evaluated the impact of an albumin-binding domain isolated from the Zag protein, a G-related protein from the surface of *Streptococcus zooepidemicus*, in the biodistribution profile of an anti-TNF VHH. Several *in vivo* studies have demonstrated the interest of fusing the ABD from streptococcal protein G to small recombinant antibody fragments to strongly extend their plasma half-lifes [7]. Results reported by Stork and co-workers also demonstrated enhancement in the blood clearance and changes on the biodistribution pattern of a single-chain diabody (scDb) directed against carcinoembryonic antigen (CEA) and CD3 capable of retargeting T cells to CEA-expressing tumor cells [20].

The VHH and VHH fused with the Zag domain were expressed in *Escherichia coli* BL21 (DE3) cells, purified using IMAC, and analyzed by SDS-PAGE. In previous studies, evaluation of binding by ELISA assays indicated that the Zag fusion protein preserved its binding to human, rat and mouse albumin as well as to TNF. Moreover, the fusion VHH-Zag presented a nanomolar affinity to human, rat and mouse serum albumin (K_d = 0.42 – 40.6 nM) as confirmed by surface plasmon resonance results [14,15].

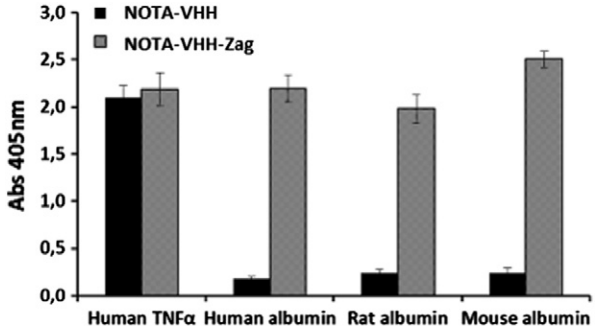

Fig. 1. Binding of the protein conjugates NOTA-VHH and NOTA-VHH-Zag to human, rat and mouse albumin, and human TNFα in ELISA assay.

Biodistribution studies with ^{99m}Tc(CO)$_3$-labelled VHH and VHH-Zag have shown that the Zag ABD fusion strategy affected the blood clearance, renal retention and excretion, as compared to the results obtained with the anti-TNF VHH [14].

The NOTA derivative p-SCN-Bn-NOTA was conjugated to the sdAbs and the resulting conjugates NOTA-VHH and NOTA-VHH-Zag were purified by gel filtration chromatography. The purity (>95%) of the conjugates was also assessed by SDS-PAGE analysis, as described for the precursor antibody fragments. The anti-TNF and the albumin-binding properties of the conjugates were assessed by ELISA (Fig. 1). The results demonstrated that the targeting properties of the antibody fragments were not affect upon conjugation to the chelator.

Radiolabeling of NOTA-VHH and NOTA-VHH-Zag with $^{67}Ga^{3+}$ was fast and efficient at room temperature. For both cases, after 5 minutes reaction, only one species (Rf = 0) was detected by ITLC-SG (Systems A and B) after gel filtration on a disposable PD10 column. Scanning of the column, after purification, in a radiochromatographer has shown negligible radioactivity retention (<5 % of the initial applied radioactivity), suggesting the absence of colloidal species and/or $^{67}GaCl_3$ precursor. Therefore, the species at the application point of the ITLC-SG chromatograms were assigned to ^{67}Ga-NOTA-VHH or ^{67}Ga-NOTA-VHH-Zag (>95% radiochemical purity).

Although we were not able to determine the number of NOTA chelators conjugated to the antibody fragments by Matrix-assisted laser desorption/ionization time-of-flight mass spectrometry (MALDI-TOF-MS), their presence was confirmed by the results of the stability studies of the radioconjugates in the presence of excess DTPA. Indeed, chromatographic analysis (ITLC-SG, systems A and B) of samples collected at different time points (2 h, 4 h, 6 h and 24 h) suggests the presence of only one species (Rf = 0), corresponding to ^{67}Ga-NOTA-VHH or ^{67}Ga-NOTA-VHH-Zag. No unreacted $^{67}GaCl_3$ precursor (System A, Rf = 1; System B, Rf = 0.4) and/or ^{67}Ga-DTPA (System B, Rf = 0.1) were detected. The presence of the latter complex would be explained by the reaction of DTPA with "free", nonspecifically bound, radiometal to the antibody during labeling. Moreover, no significant retention of radioactivity was observed in a

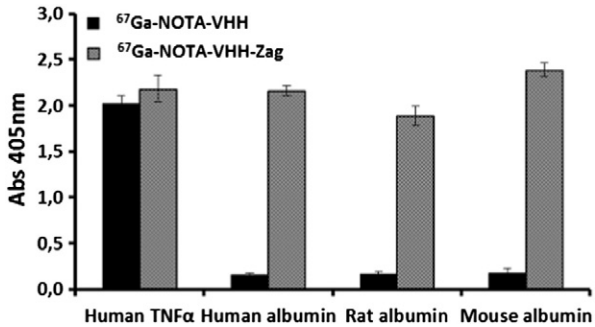

Fig. 2. Binding of ^{67}Ga-NOTA-VHH and ^{67}Ga-NOTA-VHH-Zag proteins to human, rat and mouse albumin, and human TNFα in ELISA.

Table 1
Biodistribution of ^{67}Ga-NOTA-VHH and ^{67}Ga-NOTA-VHH-ZAg in CD1- mice ($n = 3$) at 1 h, 4 h and 24 h p.i.

Organ	^{67}Ga-NOTA-VHH			^{67}Ga-NOTA-VHH-Zag		
	% I.A./g ± SD					
	1 h	4 h	24 h	1 h	4 h	24 h
Blood	**0.6 ± 0.2**	**0.16 ± 0.01**	**0.028 ± 0.004**	**8.3 ± 1.3**	**8.0 ± 2.3**	**1.7 ± 0.8**
Liver	**4.0 ± 0.7**	**6.0 ± 0.6**	**0.11 ± 0.01**	**17.6 ± 1.6**	**17.9 ± 3.6**	**20.5 ± 2.7**
Intestine	1.8 ± 0.5	1.4 ± 0.3	0.022 ± 0.005	2.9 ± 0.6	1.9 ± 0.5	1.2 ± 0.6
Spleen	0.26 ± 0.09	2.4 ± 0.3	0.041 ± 0.006	8.7 ± 2.5	11.0 ± 2.0	7.6 ± 1.8
Lung	0.8 ± 0.1	1.8 ± 0.3	0.036 ± 0.001	5.5 ± 0.3	6.6 ± 2.8	1.6 ± 0.4
Kidney	**43.5 ± 3.1**	**17.2 ± 3.0**	**4.8 ± 0.4**	**4.6 ± 1.1**	**6.1 ± 0.5**	**3.7 ± 0.3**
Muscle	0.27 ± 0.03	0.25 ± 0.19	0.010 ± 0.001	2.0 ± 0.5	2.8 ± 0.5	0.55 ± 0.01
Bone	0.26 ± 0.03	1.0 ± 0.2	0.031 ± 0.002	3.1 ± 0.4	1.6 ± 0.3	7.9 ± 1.1
Stomach	0.17 ± 0.07	0.7 ± 0.2	0.013 ± 0.002	0.27 ± 0.01	2.1 ± 0.4	0.4 ± 0.2
Total Excretion (% I.A.)	**71.3 ± 1.6**	**73.0 ± 2.9**	**97.8 ± 0.6**	**4.3 ± 1.5**	**13.6 ± 1.4**	**25.5 ± 2.1**

Radioactivity accumulation in relevant organs and total radioactivity excretion are highlighted in bold characters and numbers.

PD10 column after filtration of the stability samples, which indicates the absence of colloidal species. Therefore, the species detected at Rf = 0 could be ascribed to ^{67}Ga-NOTA-VHH or ^{67}Ga-NOTA-VHH-Zag. These results were further corroborated by the low *in vitro* stability of the radioactive species that resulted from the direct labeling of VHH and VHH-Zag with $^{67}Ga^{3+}$. Indeed, after incubation of those species with excess DTPA (2 h, 37 ºC) a significantly high degree of transchelation was observed with formation of a new species corresponding to ^{67}Ga-DTPA.

Brought together, the stability assays clearly demonstrated that the radiolabeling of the antibody fragments with $^{67}Ga^{3+}$ was achieved through NOTA complexation of the radiometal and not through unspecific binding.

The anti-TNF-binding properties of both radiolabeled antibody fragments and the albumin-binding properties of ^{67}Ga-NOTA-VHH-Zag was preserved, as indicated by ELISA assays after radioactive decay of the initial preparation (10 half-lifes) at room temperature (Fig. 2).

The *in vivo* distribution of ^{67}Ga-NOTA-VHH and ^{67}Ga-NOTA-VHH-Zag was evaluated in healthy CD-1 mice to assess the effect of the Zag domain on the pharmacokinetics profile of the radiolabelled VHH. The biodistribution results of both compounds expressed as percentage of injected activity per gram of organ (% I.A./g ± SD) is presented in Table 1. The total radioactivity excretion is also presented as percentage of the total injected activity (% I.A.).

Analysis of the biodistribution results indicated that the introduction of the Zag domain affected dramatically the pharmacokinetic properties of radiolabelled VHH, with remarkable differences in the uptake and elimination rates from major organs as well as on the excretory route. Indeed, the most striking features are the pronounced decrease in blood clearance and in the radioactivity excretion rate from the whole animal. Whereas ^{67}Ga-NOTA-VHH was rapidly cleared from the blood stream (0.6 ± 0.2% I.A./g, 0.16 ± 0.01% I.A./g, 0.028 ± 0.004% I.A./g, at 1 h, 4 h and 24 h respectively) the Zag-containing molecule ^{67}Ga-NOTA-VHH-Zag has a slow blood clearance (8.3 ± 1.3% I.A./g, 8.0 ± 2.3 % I.A./g, 1.7 ± 0.8% I.A./g, at 1 h, 4 h and 24 h respectively). ^{67}Ga-NOTA-VHH has a very rapid total excretion (approximately 70% I.A. at 1 h p.i.), mainly through the urinary pathway. On the contrary, 24 h after administration of ^{67}Ga-NOTA-VHH-Zag only 25.5 ± 2.1% I.A. was eliminated from the animal body.

The biodistribution profile of ^{67}Ga-NOTA-VHH showed a rapid clearance of the radiotracer from most tissues since no relevant radioactivity accumulation in any major organ, except those related with the excretion paths was found. Although there was a small contribution of the hepatobiliar pathway in the elimination of the radiolabelled VHH, most of the activity was rapidly taken by the kidneys and excreted into the urine. However an important amount of activity (4.8 ± 0.4%I.A./g at 24 h p.i.) was retained in this organ which is quite often a biological issue associated to radiolabelled antibody fragments and peptides. In contrast, ^{67}Ga-NOTA-VHH-Zag presented an entirely different tissue distribution. There was a slow washout not only from blood but also from muscle and bone. Moreover, due to the slowest blood clearance, highly irrigated organs such as liver, spleen, lung accumulated relevant sum of activity. The presence of ABD also shifted the excretion pathway from mainly renal to mainly hepato-biliary as indicated by the liver/kidney uptake ratio and the low excretion rate of ^{67}Ga-NOTA-VHH-Zag when compared to ^{67}Ga-NOTA-VHH. This behavior could also be partially assigned to the fact that albumin is biosynthesized in the liver, leading to a high local concentration of this protein and increased accumulation of the ABD-containing radioactive antibody fragment.

Blood samples collected from mice were analyzed by ITLC, at 1 h and 4 h p.i.. The results have shown that both ^{67}Ga-labeled antibody fragments were stable in blood serum, as no metabolites were detected after 4 h p.i. A considerable amount (>50%) of unidentified metabolites was detected by ITLC (Rf > 0) in urine samples after 4 h p.i.

4. Conclusion

In the present study we have determined the biodistribution profile of an anti-TNF antibody fragment in fusion with an ABD from Zag protein. We have shown that the fusion of this ABD can enhance the *in vivo* performance of single-domain antibodies, decreasing the blood clearance, renal retention and excretion, compared to the biodistribution profile of the unmodified antibody fragment. These findings demonstrate that the Zag fusion can be considered as a promising approach to improve the pharmacokinetics of therapeutic proteins and peptides.

Supplementary data to this article can be found online at http://dx.doi.org/10.1016/j.nucmedbio.2014.01.009.

Acknowledgments

Fundação para a Ciência e a Tecnologia (FCT), Portugal, is acknowledged for funding (project PTDC/SAU-FAR/115846/2009). C. Cantante e M. Morais thank the FCT for PhD fellowships (SFRH/BD/48598/2008 and SFRH/BD/48066/2008, respectively). We thank Dr. C. Xavier and Prof. V. Cavaliers for a generous gift of p-SCN-Bn-NOTA and fruitful discussions.

References

[1] Aires da Silva F, Corte-Real S, Goncalves J. Recombinant antibodies as therapeutic agents: pathways for modeling new biodrugs. BioDrugs 2008;22:301–14.
[2] Romer T, Leonhardt H, Rothbauer U. Engineering antibodies and proteins for molecular in vivo imaging. Curr Opin Biotechnol 2011;22:882–7.

[3] Goldsmith SJ, Signore A. An overview of the diagnostic and therapeutic use of monoclonal antibodies in medicine. Q J Nucl Med Mol Imaging 2010;54:574–81.
[4] Sharkey RM, Goldenberg DM. Perspectives on cancer therapy with radiolabeled monoclonal antibodies. J Nucl Med 2005;46(Suppl 1):115S–27S.
[5] Vaneycken I, D'Huyvetter M, Hernot S, De Vos J, Xavier C, Devoogdt N, et al. Immuno-imaging using nanobodies. Curr Opin Biotechnol 2011;22:877–81.
[6] Batra SK, Jain M, Wittel UA, Chauhan SC, Colcher D. Pharmacokinetics and biodistribution of genetically engineered antibodies. Curr Opin Biotechnol 2002;13:603–8.
[7] Kontermann RE. Strategies to extend plasma half-lives of recombinant antibodies. BioDrugs 2009;23:93–109.
[8] Kontermann RE. Strategies for extended serum half-life of protein therapeutics. Curr Opin Biotechnol 2011;22:868–76.
[9] Trussel S, Dumelin C, Frey K, Villa A, Buller F, Neri D. New Strategy for the Extension of the Serum Half-Life of Antibody Fragments. Bioconjug Chem 2009;20:2286–92.
[10] Muller C, Struthers H, Winiger C, Zhernosekov K, Schibli R. DOTA Conjugate with an Albumin-Binding Entity Enables the First Folic Acid-Targeted Lu-177-Radionuclide Tumor Therapy in Mice. J Nucl Med 2013;54:124–31.
[11] Fanali G, di Masi A, Trezza V, Marino M, Fasano M, Ascenzi P. Human serum albumin: From bench to bedside. Mol Aspects Med 2012;33:209–90.
[12] Orlova A, Jonsson A, Rosik D, Lundqvist H, Lindborg M, Abrahmsen L, et al. Site-specific radiometal labeling and improved biodistribution using ABY-027, a novel HER2-targeting affibody molecule-albumin-binding domain fusion protein. J Nucl Med 2013;54:961–8.
[13] Tolmachev V, Orlova A, Pehrson R, Galli J, Baastrup B, Andersson K, et al. Radionuclide therapy of HER2-positive microxenografts using a 177Lu-labeled HER2-specific Affibody molecule. Cancer Res 2007;67:2773–82.
[14] Cantante C, Lourenço S, Morais M, Gano L, Santos C, Fontes C, et al. Albumin-binding domain (Zag) from Streptococcus zooepidemicus increases half-life affect blood clearance of anti-TNF VHH. 8th Annual PEGS conference. Boston; 2012.
[15] Cantante C, Lourenço S, Leandro J, Morais M, Gano L, Fontes C, et al. Albumin-binding domain from Streptococcus pyogenes protein H increases half-life and affect blood clearance of anti-TNF VHH. Vienna, Austria: PEGS Europe; 2012.
[16] Jonsson H, Lindmark H, Guss B. A Protein G-Related Cell-Surface Protein in Streptococcus-Zooepidemicus. Infect Immun 1995;63:2968–75.
[17] Scasnar V, Vanlier JE. The Use of Sep-Pak Si Cartridges for the Preparation of Gallium Chloride from the Citrate Solution. Eur J Nucl Med 1993;20:273.
[18] Silence K. USA; 2007/007249 A1.
[19] Xavier C, Vaneycken I, D'huyvetter M, Heemskerk J, Keyaerts M, Vincke C, et al. Synthesis, Preclinical Validation, Dosimetry, and Toxicity of Ga-68-NOTA-Anti-HER2 Nanobodies for iPET Imaging of HER2 Receptor Expression in Cancer. J Nucl Med 2013;54:776–84.
[20] Stork R, Campigna E, Robert B, Muller D, Kontermann RE. Biodistribution of a Bispecific Single-chain Diabody and Its Half-life Extended Derivatives. J Biol Chem 2009;284:25612–9.